



The University of Bradford Institutional Repository

<http://bradscholars.brad.ac.uk>

This work is made available online in accordance with publisher policies. Please refer to the repository record for this item and our Policy Document available from the repository home page for further information.

To see the final version of this work please visit the publisher's website. Access to the published online version may require a subscription.

Link to publisher's version: <http://dx.doi.org/10.1016/j.colsurfb.2016.07.010>

Citation: Mohammad MA, Grimsey IM, Forbes RT, Blagbrough IS and Conway BR (2016) Effect of mechanical denaturation on surface free energy of protein powders. *Colloids and Surfaces B: Biointerfaces*. 146: 700-706.

Copyright statement: © 2016 Elsevier B.V. Reproduced in accordance with the publisher's self-archiving policy. This manuscript version is made available under the [CC-BY-NC-ND 4.0 license](https://creativecommons.org/licenses/by-nc-nd/4.0/)



1 **Effect of mechanical denaturation on surface free energy of protein powders**

2 Mohammad Amin Mohammad^{a,b*}, Ian M. Grimsey^a, Robert T. Forbes^a

3 Ian S. Blagbrough^c, and Barbara R Conway^d

4 ^a School of Pharmacy, University of Bradford, Bradford, BD7 1DP, UK.

5 ^b Faculty of Pharmacy, University of Damascus, Damascus, Syria.

6 ^c Department of Pharmacy and Pharmacology, University of Bath, Bath BA2 7AY, UK.

7 ^d Department of Pharmacy, University of Huddersfield, Queensgate, Huddersfield, HD1 3DH,
8 UK.

9
10
11 * Corresponding author

12 Dr. Mohammad Amin Mohammad

13 Associate Professor in Pharmaceutical Technology

14 First name: Mohammad Amin

15 Family name: Mohammad

16 Phone: + 44 (0)1225 386797

17 Email: m.a.mohammad7@bradford.ac.uk

18 Postal address: Dr. Mohammad Amin Mohammad, School of Pharmacy, University of Bradford,
19 Richmond Road, Bradford, BD7 1DP, UK.

20
21 Dr. Ian M. Grimsey, Senior Lecturer in Pharmaceutical Technology

22 Phone: +44 (0)1274 234754

23 Email: i.m.grimsey@bradford.ac.uk

24 School of Pharmacy, University of Bradford, Bradford BD7 1DP, UK

25
26 Prof. Robert T. Forbes, Professor of Biophysical Pharmaceutics

27 Phone: +44 (0)1274 234653

28 Email: r.t.forbes@bradford.ac.uk

29 School of Pharmacy, University of Bradford, Bradford BD7 1DP, UK

30
31 Dr. Ian S. Blagbrough

32 Phone: +44 (0) 1225 386795

33 Email: prsisb@bath.ac.uk

34 Department of Pharmacy and Pharmacology, University of Bath, Bath BA2 7AY, UK.

35
36 Prof. Barbara R Conway,

37 Phone: +44 (0) 1484 472347

38 Email: b.r.conway@hud.ac.uk

39 Department of Pharmacy, University of Huddersfield, Queensgate, Huddersfield, HD1 3DH,
40 UK.

46
47
48
49
50
51
52
53
54
55
56
57
58
59
60
61
62
63
64
65
66
67

ABSTRACT

Globular proteins are important both as therapeutic agents and excipients. However, their fragile native conformations can be denatured during pharmaceutical processing, which leads to modification of the surface energy of their powders and hence their performance. Lyophilized powders of hen egg-white lysozyme and β -galactosidase from *Aspergillus oryzae* were used as models to study the effects of mechanical denaturation on the surface energies of basic and acidic protein powders, respectively. Their mechanical denaturation upon milling was confirmed by the absence of their thermal unfolding transition phases and by the changes in their secondary and tertiary structures. Inverse gas chromatography detected differences between both unprocessed protein powders and the changes induced by their mechanical denaturation. The surfaces of the acidic and basic protein powders were relatively basic, however the surface acidity of β -galactosidase was higher than that of lysozyme. Also the surface of β -galactosidase powder had a higher dispersive energy compared to lysozyme. The mechanical denaturation decreased the dispersive energy and the basicity of the surfaces of both protein powders. The amino acid composition and molecular conformation of the proteins explained the surface energy data measured by inverse gas chromatography. The biological activity of mechanically denatured protein powders can either be reversible (lysozyme) or irreversible (β -galactosidase) upon hydration. Our surface data can be exploited to understand and predict the performance of protein powders within pharmaceutical dosage forms.

Keywords:

68 Protein denaturation; β -Galactosidase; Lysozyme; Conformational change; Inverse gas
69 chromatography; Surface free energy.

70 **1. Introduction**

71

72 In the pharmaceutical field, there is considerable interest in the use of globular proteins
73 for their therapeutic effects. During pharmaceutical processes, protein powders are often
74 subjected to mechanical stresses. For example, milling has been used to prepare protein particles
75 suitable for pulmonary delivery and protein-loaded microparticles in industrial quantities [1,2].
76 The mechanical stresses applied during the milling can partially or completely denature the
77 proteins and change their bulk properties [3]. In recent years, denatured globular proteins have
78 found extensive applications as excipients in pharmaceutical formulations [4,5]. Denatured
79 globular proteins have been used to prepare emulsion systems designed to enhance the
80 absorption of insoluble drugs and to form nanoparticles for drug delivery and targeting [4].
81 Globular proteins have also been successfully used to formulate controlled drug delivery tablets,
82 which delay drug release in gastric conditions by forming a gel-layer stabilized by
83 intermolecular- β sheets of denatured globular proteins [5].

84 Surface energies of powders are critical properties to be considered during formulation
85 and development of dosage forms in the pharmaceutical industry. Surface energy has significant
86 effects on pharmaceutical processes such as granulation, tableting, disintegration, dissolution,
87 dispersibility, immiscibility, wettability, adhesion, flowability, packing etc. Resultant data from
88 recent determination of surface energies have been used to reduce the time of formulation
89 development and enhance the quality of the final product [6-8].

90 The effect of the protein denaturation on their surface chemistry has been determined
91 using time-of-flight secondary ion mass spectrometry [9]. However, the effect of mechanical
92 denaturation on the surface energies of globular proteins has not been reported and these effects
93 must be understood to exploit the full potential of globular proteins in pharmaceutical industry
94 both as therapeutic agents and excipients. Inverse gas chromatography (IGC) is a useful verified
95 tool for surface energy measurements [10]. IGC has been used to measure the surface free energy
96 of lyophilized protein particles, detecting lot-to-lot variations in the amorphous microstructure of
97 lyophilized protein formulations [11].

98 This paper aims to evaluate the effects of mechanical denaturation on the surface energies
99 of globular protein powders using IGC. β -Galactosidase is a hydrolytic enzyme that has been
100 widely investigated for potential applications in the food industry to improve sweetness,
101 solubility, flavor, and digestibility of dairy products. Preparations of β galactosidases have also
102 been exploited for industrial, biotechnological, medical, and analytical applications [12].
103 Lysozyme is a naturally occurring enzyme found in bodily secretions such as tears, saliva, and
104 milk and has been explored as a food preservative and pharmaceutical. The isoelectric points (pI)
105 of β -galactosidase from *Aspergillus oryzae* and hen egg-white lysozyme are 4.6 and 11.3, and
106 were used as models of acidic and basic globular proteins, respectively [13]. Lyophilized
107 powders of these proteins were mechanically denatured by milling. Their surface energies before
108 and after denaturation were compared in order to understand how the surfaces of the globular
109 protein powders respond to the mechanical denaturation.

110

111 **2. Materials and methods**

112 *2.1. Materials*

113 *Micrococcus lysodeikticus* (Sigma-Aldrich), 2-nitrophenyl β -D-galacto pyranoside
114 (Sigma-Aldrich), lyophilized powders of β -galactosidase from *A. oryzae* (Sigma-Aldrich) and
115 hen egg-white lysozyme (Biozyme Laboratories, UK) were purchased as indicated. The
116 purchased β -galactosidase and lysozyme powders were considered to be unprocessed samples
117 and named UNG and UNL, respectively.

118

119 2.2. Preparation of mechanically denatured protein powders

120 Mechanically denatured powders of β -galactosidase and lysozyme were prepared by
121 manually milling. The milling was achieved by rotating a marble pestle over the powder within a
122 marble mortar at ~45 cycles per minute (cpm). Milling times of 60 min were enough to
123 completely denature the protein powders, and this was confirmed by differential scanning
124 calorimetry (DSC) [3]. The mechanically denatured powders of β -galactosidase and lysozyme
125 were named DeG and DeL, respectively. Three batches (2 g each batch) of the mechanically
126 denatured powders were prepared for each protein.

127

128 2.3. Microscopy

129 A Zeiss Axioplan2 polarizing microscope (Carl Zeiss Vision GmbH; Hallbergmoos,
130 Germany) was used to visualize the samples. The accompanying software (Axio Vision 4.2) was
131 then used to determine the projected area diameters of the powders.

132

133 2.4. Differential scanning calorimetry (DSC)

134 Differential scanning calorimetry (DSC) thermograms were obtained using a Perkin-
135 Elmer Series 7 DSC (Perkin-Elmer Ltd., Beaconsfield, UK). Samples (4-7 mg) were sealed in

136 aluminium pans. The escape of water was facilitated by making a pinhole in the lid prior to
137 sealing. The samples were equilibrated at 25 °C and heated to 250 °C at a scan heating rate of 10
138 °C/min under a flow of anhydrous nitrogen (20 ml/min). Each sample was analysed in triplicate.
139 The temperature axis and cell constant of the DSC cell were calibrated with indium (10 mg,
140 99.999 % pure, melting point 156.60 °C, and heat of fusion 28.40 J/g).

141

142 2.5. FT-Raman spectroscopy

143 FT-Raman spectra of samples were recorded with a Bruker IFS66 optics system using a
144 Bruker FRA 106 Raman module. The excitation source was an Nd: YAG laser operating at 1064
145 nm and a laser power of 50 mW was used. The FT-Raman module was equipped with a liquid
146 nitrogen cooled germanium diode detector with an extended spectrum band width covering the
147 wave number range 1800-450 cm^{-1} . Samples were placed in stainless steel sample cups and
148 scanned 200 times with the resolution set at 8 cm^{-1} . The observed band wave numbers were
149 calibrated against the internal laser frequency and are correct to better than $\pm 1 \text{ cm}^{-1}$. The spectra
150 were corrected for instrument response. The experiments were run at a controlled room
151 temperature of $20 \pm 1 \text{ }^\circ\text{C}$.

152

153 2.6. Enzymatic assay

154 The enzymatic activity of lysozyme samples was measured to determine the ability of
155 lysozyme to catalyze the hydrolysis of β -1,4-glycosidic linkages of cell-wall
156 mucopolysaccharides [14]. Lysozyme solution (30 μl , 0.05 % in phosphate buffer, pH = 5.2; 10
157 mM) was added to *Micrococcus lysodeikticus* suspension (2.97 ml, 0.025 % in phosphate buffer,
158 pH = 6.24; 66 mM). The decrease in the absorbance at 450 nm was monitored by using a UV-Vis

159 spectrophotometer (PU 8700, Philips, UK). The activity was determined by measuring the
160 decrease in the substrate bacterial suspension concentration with time. Hence the slope of the
161 reduction in light absorbance at 450 nm against the time of 3 min, starting when the protein
162 solutions were mixed with the substrate bacterial suspension, was considered to be the indicator
163 of the lytic activity of lysozyme [15].

164 The enzymatic activity of β -galactosidase samples was determined using a method
165 relying on the ability of β -galactosidase to hydrolyse the chromogenic substrate *o*-nitrophenyl β -
166 D-galacto pyranoside (ONPG) to *o*-nitrophenol [16]. The results were achieved by adding 20 μ l
167 of protein solution (0.05 w/v% in deionised water) to 4 ml of the substrate solution (0.665
168 mg/ml) in a phosphate buffer (100 mM and pH = 7). The mixture then was incubated for 10 min
169 in a water bath at 30 ± 1 °C. The absorbance at $\lambda = 420$ nm was measured to indicate the activity.

170 The concentrations of the protein solutions had been determined prior to the activity tests
171 using the following equation:

$$172 \quad [Protein] = Abs_{280 \text{ nm}} / E_{280 \text{ nm}} \quad (1)$$

173 where $[Protein]$ is the concentration of protein in the tested solution w/v%, $Abs_{280 \text{ nm}}$ is the
174 absorbance of the tested protein solution at 280 nm, and $E_{280 \text{ nm}}$ is the absorbance of protein
175 standard solution with concentration 0.05 w/v%. The concentrations of the solutions were diluted
176 to be about 0.05 % w/v so as to give an absorbance value of less than 0.8. The activities of all
177 samples were measured relative to that of a corresponding fresh sample, which was considered
178 as the standard solution.

179

180 2.7. Inverse gas chromatography

181 IGC experiments were performed using an inverse gas chromatography (IGC 2000,
182 Surface Measurement Systems Ltd., UK). A sample (~500 mg) was packed into a pre-silanised
183 glass column (300 mm × 3 mm i.d.). Three columns of each sample were analysed at 30 °C (the
184 lowest temperature at which the IGC experiments can be performed to avoid thermal stress) and
185 zero relative humidity, using anhydrous helium gas as the carrier. A series of n-alkanes (n-
186 hexane to n-nonane) in addition to chloroform, as a monopolar electron acceptor probe (l_+), and
187 ethyl acetate, as a monopolar donor acceptor probe (l_-), were injected through the columns at the
188 infinite dilution region. Their retention times followed from detection using a flame ionization
189 detector (FID).

190

191 2.7.1. Surface energy calculations

192 Our published methods were used to calculate the surface energies and verify their
193 accuracy [17-19]. These methods describe the surface properties using the dispersive retention
194 factor ($K_{CH_2}^a$), the electron acceptor retention factor ($K_{l_+}^a$), and the electron donor retention factor
195 ($K_{l_-}^a$), which are calculated using the retention times of probes:

196
$$\ln(t_r - t_0) = (\ln K_{CH_2}^a) n + C \quad (2)$$

197 where n is the carbon number of the homologous n-alkanes, t_r and t_0 are the retention times of
198 the n-alkanes and a non-adsorbing marker, respectively, $K_{CH_2}^a$ is the dispersive retention factor of
199 the analysed powder and C is a constant. The linear regression statistics of equation 2 generate
200 the value of t_0 which gives its best linear fit. The slope of the equation 2 gives the value of $K_{CH_2}^a$.

201
$$K_{l_+}^a = t_{nl+}/t_{nl+,ref} \quad (3)$$

202
$$K_{l_-}^a = t_{nl_-}/t_{nl_-,ref} \quad (4)$$

203 where t_{nl_+} and $t_{nl_+,ref}$ are the retention time of l_+ and its theoretical n-alkane reference,
 204 respectively, t_{nl_-} and $t_{nl_-,ref}$ are the retention time of l_- and its theoretical n-alkane reference,
 205 respectively.

206
$$\ln t_{nl_+,ref} = \ln t_{nCi} + \left(\frac{\alpha_{l_+}(\gamma_{l_+}^d)^{0.5} - \alpha_{Ci}(\gamma_{Ci}^d)^{0.5}}{\alpha_{CH_2}(\gamma_{CH_2})^{0.5}} \right) \ln K_{CH_2}^a \quad (5)$$

207
$$\ln t_{nl_-,ref} = \ln t_{nCi} + \left(\frac{\alpha_{l_-}(\gamma_{l_-}^d)^{0.5} - \alpha_{Ci}(\gamma_{Ci}^d)^{0.5}}{\alpha_{CH_2}(\gamma_{CH_2})^{0.5}} \right) \ln K_{CH_2}^a \quad (6)$$

208 where α_{CH_2} and γ_{CH_2} , α_{Ci} and γ_{Ci}^d , α_{l_+} and $\gamma_{l_+}^d$, and α_{l_-} and $\gamma_{l_-}^d$ are the cross-sectional area and
 209 the dispersive free energy of a methylene group, an n-alkane, l_+ and l_- , respectively. t_{nCi} is the
 210 retention time of the n-alkane.

211 The retention factors are then used to calculate the surface dispersive (γ_s^d), electron donor (γ_s^-)
 212 and electron acceptor (γ_s^+) components of the powders:

213
$$\gamma_s^d = \frac{0.477 (T \ln K_{CH_2}^a)^2}{(\alpha_{CH_2})^2 \gamma_{CH_2}} \text{ mJ.m}^{-2} \quad (7)$$

214
$$\gamma_s^- = \frac{0.477 (T \ln K_{l_+}^a)^2}{(\alpha_{l_+})^2 \gamma_{l_+}^+} \text{ mJ.m}^{-2} \quad (8)$$

215
$$\gamma_s^+ = \frac{0.477 (T \ln K_{l_-}^a)^2}{(\alpha_{l_-})^2 \gamma_{l_-}^-} \text{ mJ.m}^{-2} \quad (9)$$

216 where $\gamma_{l_+}^+$ is the electron acceptor component of l_+ and $\gamma_{l_-}^-$ is the electron donor component of
 217 l_- . The units of α are \AA^2 and of γ are mJ.m^{-2} in all equations.

218 The parameters of CH_2 are calculated from the following equation:

219
$$(\alpha_{CH_2})^2 \gamma_{CH_2} = - 1.869T + 1867.194 \text{ \AA}^4 \cdot \text{mJ.m}^{-2} \quad (10)$$

220 The parameters of polar probes are still under debate and different values have been
 221 reported [20-25]. In this paper, we used the values which were recently used for ethyl acetate
 222 ($\gamma_{l-}^- = 19.20 \text{ mJ/m}^2$, $\gamma_{l-}^d = 19.60 \text{ mJ/m}^2$, $\alpha_{l-} = 48.0 \text{ \AA}^2$) and for chloroform ($\gamma_{l+}^+ = 3.80 \text{ mJ/m}^2$,
 223 $\gamma_{l+}^d = 25.90 \text{ mJ/m}^2$, $\alpha_{l+} = 44.0 \text{ \AA}^2$) [17,22]. However, using any other different reported numbers
 224 will not change the findings of the comparison.

225 The percentage coefficient of variation of $\ln K_{CH_2}^a$ ($\%CV_{\ln K_{CH_2}^a}$) is the indicator of the
 226 accuracy of the surface energy measurements. The error of the slope of the equation 2
 227 ($SD_{\ln K_{CH_2}^a}$) is used to calculate $\%CV_{\ln K_{CH_2}^a}$:

$$228 \quad \%CV_{\ln K_{CH_2}^a} = \left(SD_{\ln K_{CH_2}^a} / \ln K_{CH_2}^a \right) \times 100 \quad (11)$$

229 $\%CV_{\ln K_{CH_2}^a}$ should be less than 0.7% to accept the accuracy of the measurement. $\%CV_{\ln K_{CH_2}^a}$ is then
 230 used to calculate the uncertainty range of γ_s^d :

$$231 \quad \text{Uncertainty Range of } \gamma_s^d = \left[\left(\frac{100 \times \gamma_s^d}{100 + 7.5\% CV_{\ln K_{CH_2}^a}} \right) \text{ to } \left(\frac{100 \times \gamma_s^d}{100 - 7.5\% CV_{\ln K_{CH_2}^a}} \right) \right] \quad (12)$$

232

233 3. Results and discussion

234 3.1. Microscopy

235 The photomicrographs of UNL, UNG, DeL, and DeG powders show that they had
 236 project-area diameters of $\sim 4 \text{ }\mu\text{m}$ (Fig. S1), $\sim 2.5 \text{ }\mu\text{m}$ (Fig. S2), $\sim 1.5 \text{ }\mu\text{m}$ (Fig. S3), and $\sim 1.5 \text{ }\mu\text{m}$
 237 (Fig. S4), respectively. The particle sizes of the original powders were below $5 \text{ }\mu\text{m}$. Therefore,
 238 the attrition mechanism was dominant during milling, and so the same original faces did not
 239 change [3].

240

241 3.2. Differential scanning calorimetry (DSC)

242 For both proteins, DSC thermograms exhibited broad peaks ranging from ~30 to ~140 °C
243 (Figure 1). These peaks are due to water removal, and their areas depend on water residues in the
244 powders [3]. The enthalpy of the water evaporation peak was 118 ± 11 , 124 ± 6 , 114 ± 9 and 130 ± 8
245 J/g for UNL, UNG, DeL, and DeG, respectively, and did not significantly change after milling (t-
246 test: $P < 0.05$). The protein powders exchange water with the surrounding air depending on
247 conditions of temperature, relative humidity and exposure time. Therefore, the conditions used
248 during milling did not change the water content of the powders. Also Figure 1 shows that the
249 unprocessed proteins unfolded and a peak was detected at their apparent denaturation
250 temperatures, which varied according to the protein. DSC thermograms of UNL displayed one
251 denaturation peak at ~201 °C, but UNG displayed two denaturation peaks at ~176 °C and ~212
252 °C.
253

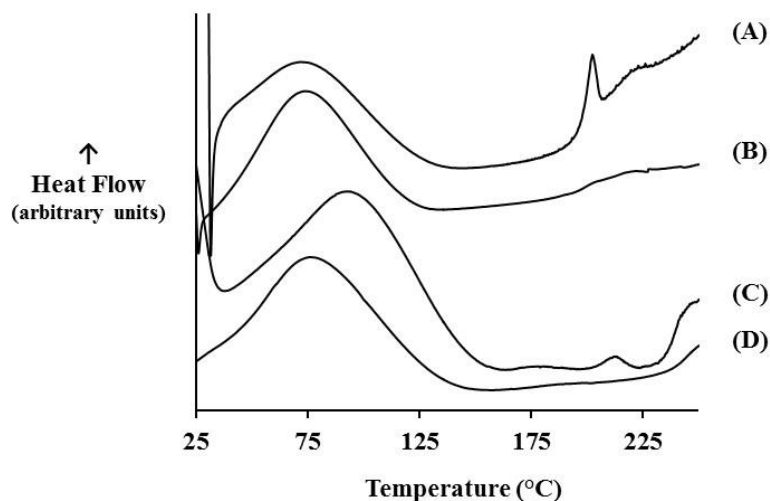


Fig. 1. Example DSC thermograms of protein powders (A) unprocessed lysozyme, (B) mechanically denatured lysozyme, (C) unprocessed β -galactosidase, (D) mechanically denatured β -galactosidase. Conditions: samples heated from 25 to 250 °C; heating rate: 10 °C/min.

254

255 The difference in the thermal denaturation pattern can be due to the difference in the
256 thermal unfolding mechanisms of the proteins. While lysozyme folds in a highly cooperative
257 manner and so exhibits an all-or-none thermal unfolding transition, β -galactosidase goes through
258 a non-two state thermal unfolding transition resulting in two peaks [26,27]. The unfolding
259 transition peaks were completely lost after mechanical denaturation. Hence there was no peak at
260 ~ 201 °C for the milled lysozyme samples and neither were there peaks at ~ 176 °C and ~ 212 °C
261 for the milled β -galactosidase. The complete disappearance of the unfolding transition peak from
262 the DSC thermogram indicates the total transition of the protein from its folded state to its
263 unfolded state [3].

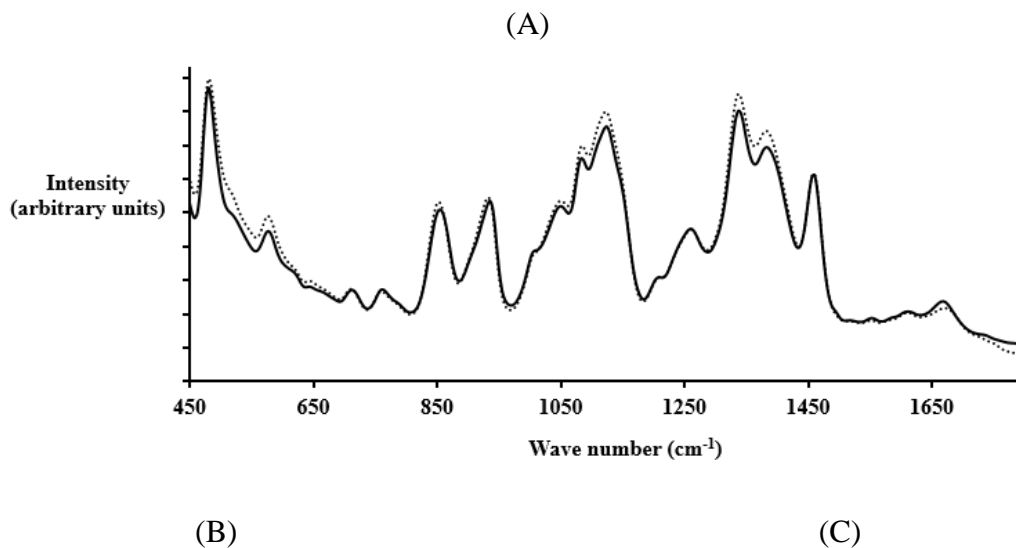
264

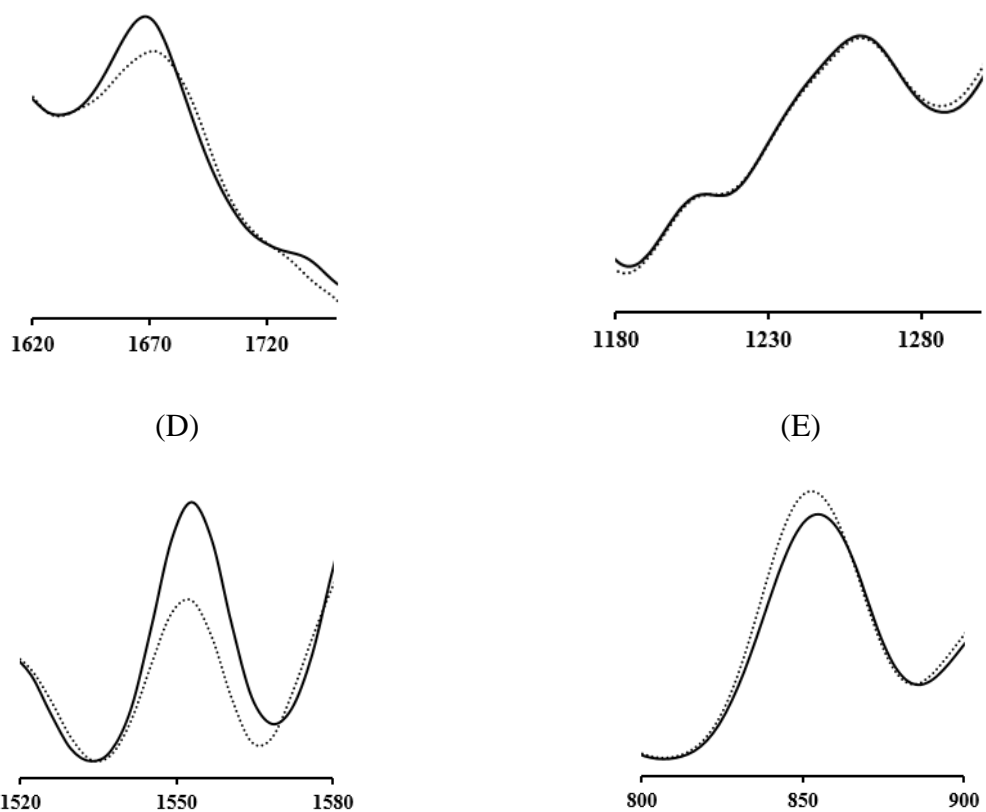
265 *3.3. FT-Raman study*

266 Raman spectroscopy was used to compare the molecular conformation of protein
267 powders before and after mechanical denaturation. The band at ~ 1450 cm^{-1} indicates the CH
268 bending vibrations of aliphatic side chains, and its intensity and position are unaffected by
269 changes induced in protein structure after dehydration or applying different stresses [28].
270 Therefore, it was used as an internal intensity standard to normalize Raman spectra before
271 comparison (Figures 2A and 3A). The vibration modes of amide I (C=O stretch) from 1580 to
272 1720 cm^{-1} (Figures 2B and 3B) and amide III (N-H in-plane bend + C-N stretch) from 1250–
273 1330 cm^{-1} (Figures 2C and 3C) demonstrated the secondary structure of β -galactosidase and
274 lysozyme, respectively. The spectra of the denatured samples show that the modes of the amide I
275 upshifted and broadened for both proteins, and the mode of the amide III intensified and

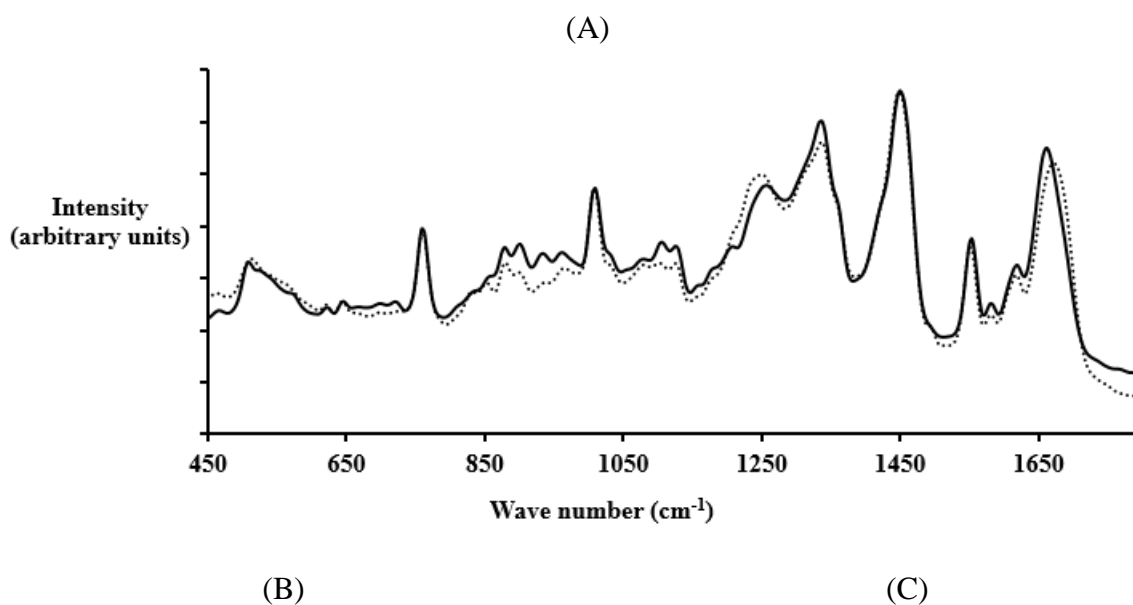
276 downshifted, especially for lysozyme, but there was no change in the mode of amide III for β -
277 galactosidase. These changes indicated the transformation of α -helix content to β -sheets or a
278 disordered structure which enhances the tendency of proteins to aggregate [3,29]. While β -
279 galactosidase is a beta-type protein containing mainly β -sheet structure and only 5% α -helix [30],
280 the secondary structure of lysozyme consists of 30% α -helix [31]. This explains why no changes
281 in the amide III of β -galactosidase were observed.

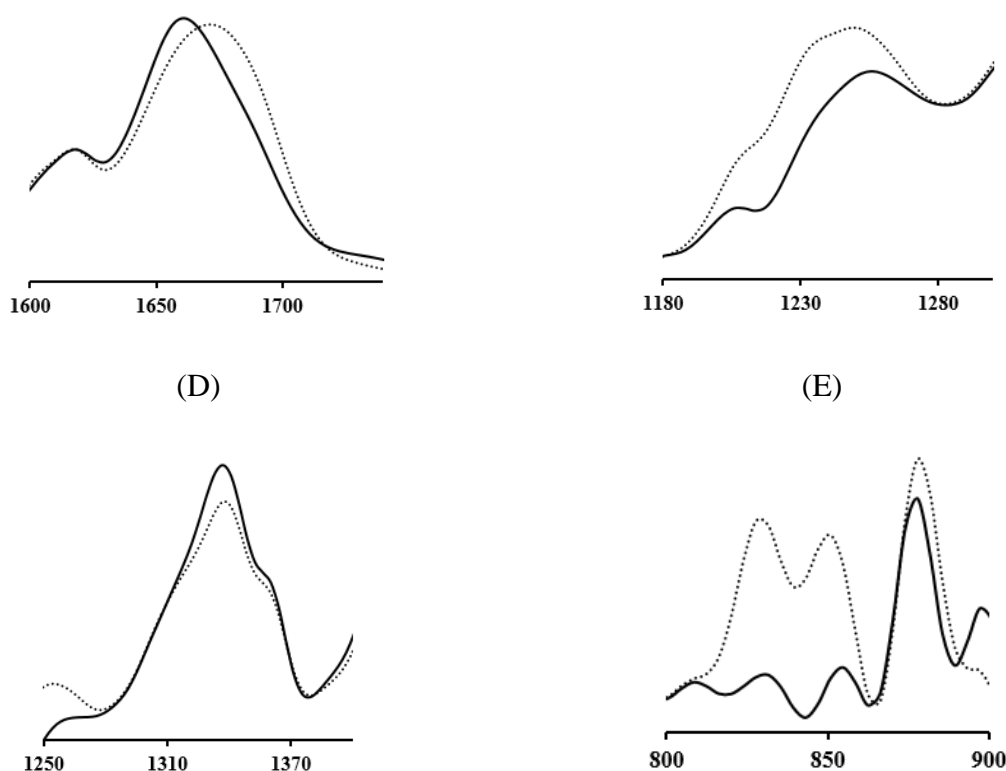
282 The aggregation of denatured proteins combined with changes in the vibration modes of
283 the aromatic residues at $\sim 1550\text{ cm}^{-1}$ in β -galactosidase (Figure 2D), $1320\text{-}1380\text{ cm}^{-1}$ in lysozyme
284 (Figure 3D) and $800\text{-}900\text{ cm}^{-1}$ in both proteins (Figures 2E and 3E). These changes in the
285 vibration modes of the aromatic residues result from the changes in their micro-environment
286 after denaturation because of their roles in the denaturation processes [29,32]. The aggregates of
287 denatured protein molecules are formed via π -stacking interactions of the aromatic residues [33].





288 **Fig. 2.** FT-Raman spectra of β -galactosidase powders, the unprocessed powders (solid lines) and
 289 the mechanically denatured powders (dotted lines). Vibration modes of secondary structure are
 290 (B) amide I and (C) amide III. Vibration modes of tertiary structure are (D) for Trp and (E) for
 291 Trp and Tyr. The spectra were normalized using the methylene deformation mode at $\sim 1450\text{ cm}^{-1}$
 292 as an internal intensity standard.
 293





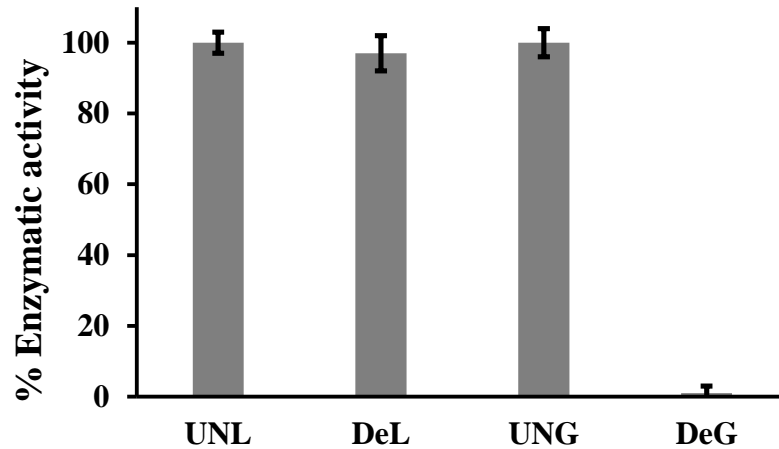
294 **Fig. 3.** FT-Raman spectra of lysozyme powders, the unprocessed powders (solid lines) and the
 295 mechanically denatured powders (dotted lines). Vibration modes of secondary structure are (B)
 296 amide I and (C) amide III. Vibration modes of tertiary structure are (D) for Trp and (E) for Trp
 297 and Tyr. The spectra were normalized using the methylene deformation mode at $\sim 1450\text{ cm}^{-1}$ as
 298 an internal intensity standard.
 299

300 3.4. Enzymatic assay

301 Therapeutic proteins may rapidly denature and lose their enzymatic activity. The
 302 structure changes detected using FT-Raman and the absence of T_m detected by DSC have been
 303 used to monitor the denaturation of proteins, and the results of Raman and DSC are linked to the
 304 results of enzymatic activity [34]. Our DSC and Raman results confirmed the denaturation of
 305 both proteins studied. The enzymatic assay showed that the mechanically denatured β -
 306 galactosidase samples (DeG) demonstrated no enzymatic activity (Figure 4). However, the
 307 mechanically denatured lysozyme samples (DeL) maintained full enzymatic activity when

308 compared to an unprocessed sample (t-test: $P < 0.05$) (Figure 4). This is due to the ability of
309 denatured lysozyme to refold upon dissolution in aqueous media and thus the biological activity
310 of lysozyme is fully recovered following dissolution [3.35].

311



312

313 **Fig. 4. Enzymatic activity of the unprocessed powders and the mechanically**
314 **denatured powders of lysozyme and β -galactosidase.**

315

316 3.5. Surface free energy

317 The IGC results (Table 1) confirm the acceptable accuracy of the IGC experiments
318 considered in this work with $\%CV_{\ln K_{CH_2}^a}$ values of less than 0.7% [18]. IGC data for the
319 unprocessed powders demonstrated the differences in the surface free energy between β -
320 galactosidase (an acidic protein) and lysozyme (a basic protein). UNG had higher γ_s^d compared to
321 UNL because the uncertainty ranges of γ_s^d of UNG and UNL did not overlap for the three
322 columns [18]. The surface acidity (γ_s^+) and the surface basicity (γ_s^-) of UNG were significantly
323 different from their counterparts of UNL (t-test: $P < 0.05$). The average of γ_s^+ was 16.2 ± 0.2 and
324 12.4 ± 0.1 mJ.m^{-2} and the average of γ_s^- was 5.5 ± 0.2 and 10.5 ± 0.6 mJ.m^{-2} for UNG and UNL,

325 respectively. This proves that UNG, chosen as a model for acidic proteins, has higher surface
 326 acidity and lower surface basicity compared to selected basic protein, UNL.

327

328 **Table 1.** The surface energies (γ_s^d , γ_s^+ and γ_s^-) and retention factors ($K_{CH_2}^a$, K_{l+}^a and K_{l-}^a) of the
 329 lyophilized lysozyme powder (UNL), the lyophilized β -galactosidase powder (UNG), the
 330 mechanically denatured lyophilized lysozyme powder (DeL) and the mechanically denatured
 331 lyophilized β -galactosidase powder (DeG).

Material	Column	$K_{CH_2}^a$	K_{l+}^a	K_{l-}^a	$\%CV_{\ln K_{CH_2}^a}$	γ_s^d mJ.m ⁻²	Uncertainty Range of γ_s^d mJ.m ⁻²	γ_s^+ mJ.m ⁻²	γ_s^- mJ.m ⁻²
UNL	1	3.099	3.725	34.572	0.144	43.1	41.9-44.4	12.4	10.3
UNL	2	3.095	3.677	34.668	0.094	43.0	42.2-43.9	12.5	10.1
UNL	3	3.089	3.944	33.704	0.077	42.9	42.2-43.6	12.3	11.2
DeL	1	2.937	2.781	33.948	0.127	39.1	38.1-40.2	12.3	6.2
DeL	2	2.965	2.742	31.928	0.147	39.8	38.7-41.0	11.9	6.1
DeL	3	2.944	2.801	31.826	0.117	39.3	38.4-40.3	11.9	6.3
UNG	1	3.235	2.542	55.641	0.141	46.5	45.1-47.8	16.0	5.2
UNG	2	3.222	2.640	58.508	0.076	46.1	45.4-46.9	16.4	5.6
UNG	3	3.228	2.625	56.028	0.158	46.3	44.8-47.9	16.1	5.6
DeG	1	2.926	1.980	43.387	0.205	38.9	37.3-40.6	14.1	2.8
DeG	2	2.958	1.829	41.065	0.160	39.7	38.4-41.0	13.7	2.2
DeG	3	2.948	1.841	39.710	0.221	39.4	37.7-41.3	13.4	2.2

332

333 The isoelectric point (pI) of a protein indicates its relative acidity or basicity, the higher
 334 the pI, the higher the basicity of the molecule [36]. The isoelectric points (pI) of the β -
 335 galactosidase and lysozyme used are 4.6 and 11.3, respectively [13]. The molecule of β -
 336 galactosidase contains ~11 w/w% basic amino acids (histidine, lysine, and arginine) and ~22
 337 w/w% acidic (aspartic acid and glutamic acid) residues [37], i.e., approximately double the
 338 number of acidic groups compared to basic. Conversely the lysozyme contains ~18 w/w% and
 339 ~7 w/w% basic (histidine, lysine, and arginine) and acidic (aspartic acid and glutamic acid)
 340 residues, respectively [38]. [Detailed information regarding](#) the structures of β -galactosidase and
 341 lysozyme can be found in [37,38]. However, this is not the only determinant of energy as the
 342 surfaces of both the acidic (UNG) and basic (UNL) protein powders were relatively basic (the

343 values of $\gamma_s^+ > \gamma_s^-$). Therefore to explain our results further, the interaction of protein molecules
344 with surfaces and interfaces, during preparation using lyophilization technique, must be
345 considered.

346 As protein molecules are surface active containing both polar and nonpolar groups, they
347 tend to adsorb to interfaces via hydrophobic interactions (London), coulombs (electrostatic)
348 and/or hydrogen bonding, and they reorient their surfaces to the parts which give the optimum
349 attractive force and the most stable state (minimum energy) with a substrate or an interface [39].
350 Upon lyophilization, protein molecules adsorb to the formed ice via hydrophobic residues but not
351 via hydrophilic residues, and this gives support to the hypothesis that the interaction of proteins
352 with ice involves appreciable hydrophobic interactions [40]. The hydrophobic regions in protein
353 molecules interact spontaneously with the ice faces by an entropy driving force [41]. The rich
354 electron rings of aromatic residues orient so that the ring structures lie flat with the interface in
355 order to maximize the interaction at interfaces and lower the Gibbs free energy of the system
356 [42]. Therefore, lyophilized protein particles expose the rich electron rings of the aromatic
357 residues on their surfaces. Aromatic groups, via their π electrons, which are considered
358 nucleophilic, can form hydrogen bonds with chemical groups (acidic polar probes) being the
359 hydrogen donors [43]. Therefore, exposing these rings to surfaces relatively increases their
360 basicity compared to their acidity irrespective of the acidic or basic nature of the proteins
361 themselves. Also the ring structures can participate in raising the dispersive surface energy via
362 London interactions due to their high polarizability [43]. The aromatic residues (tryptophan,
363 tyrosine, and phenylalanine) make up 16%w/w of the β -galactosidase molecules and 14%w/w of
364 the lysozyme molecules [37,38]. This explains the higher values of γ_s^d of β -galactosidase
365 compared to lysozyme, prior to mechanical denaturation.

366 UNG was more acidic than UNL. The size and the shape of the molecule can also
367 influence orientation. UNG is larger than UNL, with a globular shape and when some of the
368 chemical groups are preferably exposed to a surface (energetically or entropically), this will
369 expose not only those specific groups but also other closely associated groups which will vary in
370 nature from one protein to another.. Thus, the surfaces of the acidic protein (β -galactosidase)
371 were more acidic compared to the basic protein (lysozyme).

372 Table 1 shows that mechanical denaturation decreased the dispersive free energy and the basicity
373 of the surfaces of protein powders, irrespective of the nature of the protein (acidic or basic).
374 Usually milling induces an increase in the dispersive energy due to the generation of surface
375 amorphous regions or/and creation of higher energy crystal faces because of particle
376 fracture/breakage, thus the surface acidity and basicity change according to the formation of new
377 faces and regions [44,45]. However, in our case, due to lyophilization, the protein powders are
378 amorphous with particle sizes below 5 μm . Therefore, there would be no further size reduction
379 by fracture mechanisms because of brittle ductile transition [3]. Therefore, the denatured protein
380 powders were produced by milling where the attrition mechanism was dominant and so the same
381 original faces did not change. During milling, the extensive mechanical energy completely
382 denatured the protein molecules as confirmed by DSC and Raman results. This denaturation led
383 to aggregation of the protein molecules via non-covalent interactions through π -stacking
384 interactions [33]. This caused a loss of the aromatic groups, which are rich in π electrons, from
385 the surfaces. Therefore, a decrease in the Van der Waals interactions, a major contributor to
386 dispersive energy and nucleophilicity (basicity) occurred, and so γ_s^d and γ_s^- decreased after
387 denaturation for both proteins. Also this loss of aromatic residues from the surface of the
388 denatured powders renders γ_s^d similar for both proteins. This is further evidence that the exposed

389 aromatic residues raise the γ_s^d as outlined previously. The Raman spectroscopic results confirmed
390 that the aromatic residues were involved in the denaturation processes, therefore, supporting the
391 findings and our interpretation of the IGC studies.

392 **4. Conclusions**

393 The surface energies of the lyophilized protein powders differed according to their amino
394 acid compositions. The absence of the thermal unfolding transition phase for the proteins
395 (lysozyme and β -galactosidase) and the changes in the conformation of the back-bone and side
396 chains confirmed that the mechanical milling process caused denaturation of the protein
397 powders, and this denaturation could potentially be reversible in solution. The acidic protein
398 powder (β -galactosidase) had higher surface acidity (γ_s^+) and lower surface basicity (γ_s^-)
399 compared to the basic protein powder (lysozyme). However, both protein powders had relatively
400 basic surfaces due to the rich electron rings of the aromatic residues which are nucleophilic.
401 During mechanical denaturation, these rings tend to associate through π -stacking interactions and
402 are thus concealed from the surface. Their removal reduced γ_s^- and γ_s^d of the surfaces of both
403 protein powders, and thereby yielded similar γ_s^d for the surfaces of both proteins.

404

405 **Acknowledgements**

406 MAM gratefully acknowledges CARA (Stephen Wordsworth and Ryan Mundy) the Universities
407 of Bath and Bradford for providing academic fellowships.

408

409 **Supplementary data**

410 Supplementary data associated with this article can be found, in the online version, at
411 <http://dx.doi.org/XXXX>.

412
413
414
415
416
417
418
419
420
421
422
423
424
425
426
427
428
429
430
431
432
433
434
435
436
437
438
439
440
441
442
443
444
445
446
447
448
449
450
451
452
453
454
455
456

References

- [1] H. Hoyer, W. Schlocker, K. Krum, A. Bernkop-Schnürch, *Eur. J. Pharm. Biopharm.* 69 (2008) 476.
- [2] W. Schlocker, S. Gschliesser, A. Bernkop-Schnürch, *Eur. J. Pharm. Biopharm.* 62 (2006) 260.
- [3] M.A. Mohammad, I.M. Grimsey, R.T. Forbes, *J. Pharm. Biomed. Anal.* 114 (2015) 176.
- [4] W. He, K. Yang, L. Fan, Y. Lv, Z. Jin, S. Zhu, C. Qin, Y. Wang, L. Yin, *Int. J. Pharm.* 495 (2015) 9.
- [5] R. Caillard, M. Subirade, *Int. J. Pharm.* 437 (2012) 130.
- [6] V. Karde, C. Ghoroi, *Int. J. Pharm.* 475 (2014) 351.
- [7] X. Han, L. Jallo, D. To, C. Ghoroi, R. Davé, *J. Pharm. Sci.* 102 (2013) 2282.
- [8] D. Cline, R. Dalby, *Pharm. Res.* 19 (2002) 1274.
- [9] M.S. Killian, H.M. Krebs, P. Schmuki, *Langmuir* 27 (2011) 7510.
- [10] O. Planinsek, A. Trojak, S. Srcic, *Int. J. Pharm.* 221 (2001) 211.
- [11] Y. Hirakura, H. Yamaguchi, M. Mizuno, H. Miyanishi, S. Ueda, S. Kitamura, *Int. J. Pharm.* 340 (2007) 34.
- [12] Q. Husain, *Crit. Rev. Biotechnol.* 30 (2010) 41.
- [13] M. Ospinal-Jiménez, D.C. Pozzo, *Langmuir* 28 (2012) 17749.
- [14] R.R. Haj-Ahmad, A.A. Elkordy, C.S. Chaw, A. Moore, *Eur. J. Pharm. Sci.* 49 (2013) 519.
- [15] S. Chakraborti, T. Chatterjee, P. Joshi, A. Poddar, B. Bhattacharyya, S.P. Singh, V. Gupta, P. Chakrabarti, *Langmuir* 26 (2010) 3506.
- [16] R.E. Hamlin, T.L. Dayton, L.E. Johnson, M.S. Johal, *Langmuir* 23 (2007) 4432.
- [17] M.A. Mohammad, *J. Chromatogr. A* 1318 (2013) 270.
- [18] M.A. Mohammad, *J. Chromatogr. A* 1399 (2015) 88.
- [19] M.A. Mohammad, *J. Chromatogr. A* 1408 (2015) 267.
- [20] B. Shi, D. Qi, *J. Chromatogr. A* 1231 (2012) 73.
- [21] C. Della Volpe, D. Maniglio, M. Brugnara, S. Siboni, M. Morra, *J. Colloid Interface Sci.* 271 (2004) 434.
- [22] S.C. Das, I. Larson, D.A. Morton, P.J. Stewart, *Langmuir* 27 (2011) 521.
- [23] C.D. Volpe, S. Siboni, *J. Colloid Interface Sci.* 195 (1997) 121.
- [24] J. Schultz, L. Lavielle, C. Martin, *J. Adhesion* 23 (1987) 45.
- [25] C.J. Van Oss, R.J. Good, M.K. Chaudhury, *Langmuir* 4 (1988) 884.
- [26] B. Maroufi, B. Ranjbar, K. Khajeh, H. Naderi-Manesh, H. Yaghoubi, *Biochim. Biophys. Acta* 1784 (2008) 1043.
- [27] J.M. Sánchez, V. Nolan, M.A. Perillo, *Colloids Surf. B Biointerfaces* 108 (2013) 1.
- [28] T.J. Yu, J.L. Lippert, W.L. Peticolas, *Biopolymers* 12 (1973) 2161.
- [29] E.N. Lewis, W. Qi, L.H. Kidder, S. Amin, S.M. Kenyon, S. Blake, *Molecules* 19 (2014) 20888.
- [30] S.R. Tello-Solís, J. Jiménez-Guzmán, C. Sarabia-Leos, L. Gómez-Ruíz, A.E. Cruz-Guerrero, G.M. Rodríguez-Serrano, M. García-Garibay, *J. Agric. Food Chem.* 53 (2005) 10200.

- 457 [31] P.J. Artymiuk, C.C.F. Blake, D.W. Rice, K.S. Wilson, *Acta Crystallogr. B: Struct.*
458 *Crystallogr. Cryst. Chem.* B38 (1982) 778.
- 459 [32] C. Zhou, W. Qi, E.N. Lewis, J.F. Carpenter, *Anal. Biochem.* 472 (2015) 7.
- 460 [33] S. Jang, J. Jang, W. Choe, S. Lee, *ACS Appl. Mater. Interfaces* 7 (2015) 1250.
- 461 [34] A. Torreggiani, M. Di Foggia, I. Manco, A. De Maio, S.A. Markarian, S. Bonora, *J. Mol.*
462 *Struct.* 891 (2008) 115.
- 463 [35] A. Torreggiani, M. Tamba, I. Manco, M.R. Faraone-Mennella, C. Ferreri, C. Chatgialoglu,
464 *J. Mol. Struct.* 744 (2005) 767.
- 465 [36] C. Sun, J.C. Berg, *Adv. Colloid Interface Sci.* 105 (2003) 151.
- 466 [37] Y. Tanaka, A. Kagamiishi, A. Kiuchi, T. Horiuchi, *J. Biochem.* 77 (1975) 241.
- 467 [38] M.C. Vaney, S. Maignan, M. Riès-Kautt, A. Ducriux, *Acta Crystallogr. D. Biol. Crystallogr.*
468 52 (1996) 505.
- 469 [39] C. Chaiyasut, Y. Takatsu, S. Kitagawa, T. Tsuda, *Electrophoresis* 22 (2001) 1267.
- 470 [40] J. Baardsnes, P.L. Davies, *Biochim Biophys Acta.* 160 (2002) 49.
- 471 [41] S. Pezennec, F. Gauthier, C. Alonso, F. Graner, T. Croguennec, G. Brulé, A. Renault, *Food*
472 *Hydrocolloids* 14 (2000) 463.
- 473 [42] M. Jurkiewicz-Herbich, A. Muszalska, R. Słojkowska, *Colloids Surfaces A: Physicochem.*
474 *Eng. Aspects* 131 (1998) 315.
- 475 [43] G.I. Makhatadze, P.L. Privalov, *Biophys. Chem.* 50 (1994) 285.
- 476 [44] U.V. Shah, Z. Wang, D. Olusanmi, A.S. Narang, M.A. Hussain, M.J. Tobyn, J.Y. Heng, *Int.*
477 *J. Pharm.* 495 (2015) 234.
- 478 [45] X. Han, L. Jallo, D. To, C. Ghoroi, R. Davé, *J. Pharm. Sci.* 102 (2013) 2282.